İSTANBUL TECHNICAL UNIVERSITY ★ INSTITUTE OF SCIENCE AND TECHNOLOGY

DESIGN AND PERFORMANCE ANALYSIS OF A MINI UNMANNED COAXIAL HELICOPTER

M.Sc. Thesis by

Belkıs ERZİNCANLI, B.Sc.

Department: Advanced Technologies in Engineering

Programme: Aeronautics and Astronautics Engineering

JANUARY 2008

İSTANBUL TECHNICAL UNIVERSITY ★ INSTITUTE OF SCIENCE AND TECHNOLOGY

DESIGN AND PERFORMANCE ANALYSIS OF A MINI UNMANNED COAXIAL HELICOPTER

M.Sc. Thesis by

Belkıs ERZİNCANLI, B.Sc.

Department: Advanced Technologies in Engineering

Programme: Aeronautics and Astronautics Engineering

JANUARY 2008

İSTANBUL TECHNICAL UNIVERSITY ★ INSTITUTE OF SCIENCE AND TECHNOLOGY

DESIGN AND PERFORMANCE ANALYSIS OF A MINI UNMANNED COAXIAL HELICOPTER

M.Sc. Thesis by

Belkıs ERZİNCANLI, B.Sc.

(521051102)

Date of submission : 24 December 2007

Date of defence examination : 28 January 2008

Supervisor (Chairman): **Prof. Dr. A. Rüstem ASLAN (İTÜ)**

Members of the Examining Committee **Prof.Dr. Aydın MISIRLIOĞLU (İTÜ)**

Assist. Prof.Dr. Gökhan İNALHAN (İTÜ)

JANUARY 2008

İSTANBUL TEKNİK ÜNİVERSİTESİ ★ FEN BİLİMLERİ ENSTİTÜSÜ

İNSANSIZ EŞEKSENLİ MİNİ HELİKOPTERİN TASARIM VE PERFORMANS ANALİZİ

YÜKSEK LİSANS TEZİ

Belkıs ERZİNCANLI

(521051102)

Tezin Enstitüye Verildiği Tarih : 24 Aralık 2007

Tezin Savunulduğu Tarih : 28 Ocak 2008

Tez Danışmanı : Prof. Dr. A. Rüstem ASLAN (İTÜ)

Diğer Jüri Üyeleri : Prof.Dr. Aydın MISIRLIOĞLU (İTÜ)

Yard. Doç. Dr. Gökhan İNALHAN (İTÜ)

OCAK 2008

PREFACE

I would like to extend my gratitude to the following people for their contributions to this research: to Prof. Dr. A. Rüstem Aslan for being my graduate advisor, Research Assistant Murat Bronz for teaching me so many things and providing guidance and advice for my research, ROTAM technician Aytekin Güven for helping with manufacturing and preparations for experimental tests.

And special thanks to my family for their endless support during my life.

January, 2008 **BELKIS ERZİNCANLI**

INDEX

ABBREVIATIONS

COTS **:** Commercial Off-The-Shelf

RPM **:** Revolutions per Minute

UAV **:** Unmanned Air Vehicle

ROTAM **:** Rotorlu Araçlar Tasarım ve Mükemmeliyet Merkezi

ESC **:** Electronic Speed Controller

LIST OF TABLES

Page Number

LIST OF FIGURES

Page Number

NOMENCLATURE

A	**:** Rotor disk area, [m^2]
c	**:** Chord length, [m]
$\mathbf{r_{co}}$	**:** Non dimensional blade root cut-out (fraction of R)
$\mathbf{C_L}$	**:** Lift coefficient
$\mathbf{C_T}$	**:** Thrust coefficient
FM	**:** Rotor Figure of Merit
k	**:** Rotor induced power constant
m	**:** Mass flow rate
$\mathbf{M_{Tip}}$	**:** Tip Mach number
n	**:** Number of blade elements
N	**:** Number of blades
P	**:** Rotor power, [N]
Q	**:** Rotor shaft torque, [Nm]
r	**:** Radial position
R	**:** Rotor radius, [m]
T	**:** Rotor thrust, [N]
$\mathbf{v_l}$	: Induced velocity of the lower rotor, [m/s]
$\mathbf{v_u}$	**:** Induced velocity of the upper rotor, [m/s]
w	**:** Induced velocity at the wake, [m/s]
$\mathbf{C_{L\alpha}}$	**:** Lift curve slope
α	**:** Angle of attack, [rad]
σ	**:** Solidity ratio
ρ	**:** Density of air, [kg/m^3]
θ	**:** Blade pitch angle
λ	**:** Inflow ratio
$\theta_{0,75}$	**:** Rotor collective, blade pitch angle at 75% rotor radius
θ_{tw}	**:** Linear twist rate of blades, [deg]
Ω	**:** Rotor speed, [rad/s]

DESIGN AND PERFORMANCE ANALYSIS OF A MINI UNMANNED COAXIAL HELICOPTER

SUMMARY

This thesis presents the design of a mini unmanned coaxial helicopter which can be used for indoor mission as a safe and military scouting device. Since a mini rotary wing air vehicle has a small size, and the ability to hover, it can approach rugged or dangerous areas where human can not go. The primary goal of the design is to develop a mini unmanned coaxial helicopter which could carry the maximum payload for the specified maximum gross weight, taking real time images in a building. The main reason of selecting coaxial rotor configuration is that it allows the aircraft remain small in size due to removal of a tail rotor and boom. The study focuses on conceptual and preliminary design, power system and stability and control. For the aerodynamic analysis of each blade, "Momentum Theory" and "Blade Element Momentum Theory" are used. The preliminary design is done by using the "Momentum Theory" and is supported by the results of the "Blade Element Momentum Theory". The vehicle designed in this study, consists of coaxial rotor blades, electronic speed controller, gyroscope, electric motor, battery, camera, and other systems. Propulsion is provided by a combination of an electric brushless outrunner motor and a high capacity lithium polymer battery pack. A small camera is used for optical surveillance. The gross weight of the vehicle is 2000 grams and the (desired) endurance is 30 minutes. As a result, the conceptual and preliminary designs are carried out. The body of the helicopter is constructed and COTS components are procured. Further study will focus on the fabrication of the prototype according to the desired characteristics. Also, the system integration, ground and flight tests will be performed.

İNSANSIZ EŞEKSENLİ MİNİ HELİKOPTERİN TASARIM VE PERFORMANS ANALİZİ

ÖZET

Bu çalışmada, insansız eşeksenli mini helikopterin tasarımı sunulmaktadır. Döner kanatlı mini hava aracı küçük boyutlu olduğu ve askıda kalabilme yeteneğine sahip olduğu için insanların giremediği engebeli ve tehlikeli yerlere ulaşabilmektedir. Çalışmanın öncelikli amacı belirlenmiş maksimum ağırlıkla maksimum paralı yük taşıyabilecek ve bir binada gerçek zamanlı görüntü alabilecek insansız eşeksenli mini bir helikopter geliştirmektir. Eşeksenli rotor konfigurasyonunun seçilmesinin temel nedeni bu konfigurasyonun kuyruk ve kuruk rotoru içermemesi nedeniyle aracın küçük boyutlarda kalmasına olanak vermesidir. Çalışmada özellikle kavramsal ve ön tasarım, güç sistemi, kararlılık ve kontrol konuları üzerinde durulmaktadır. Her bir palanın aerodinamik tasarımı için Momentum Kuramı ve Pala Elemanı Momentum Kuramı kulalnılmaktadır. Ön tasarım, Momentum Kuramı kullanılarak ve Pala Elemanı Momentum Kuramı sonuçlarıyla desteklenerek yapılmıştır. Bu çalışmada tasarlanan helikopter; rotor (döneç) palaları, elektronik hız kontrolörü, jiroskop, elektrik motoru, pil, kamera ve diğer sistemlerden oluşmaktadır. İtici güç, fırçasız elektrik motor ve yüksek kapasiteli lityum polimer pil paketinin birleşmesiyle sağlanmaktadır. Optik gözlem için küçük bir kamera kullanılmaktadır. Aracın toplam ağırlığı 2000 gram ve istenen takat 30 dakikadır. Sonuç olarak, kavramsal ve ön tasarım yapılmıştır. Helikopterin gövdesi yapılmakta ve bazı parçaları hazır satın alınarak temin edilmektedir. İleriki çalışmada istenen özelliklere sahip prototipin üretimi yapılacaktır. Bunun yanısıra, sistem entegrasyonu, yer ve uçuş testleri de yapılacaktır.

1. INTRODUCTION

Along the way of helicopter design, there have been attempts to design a helicopter which has improved stability and control characteristics, streamlined design with reduced drag and hence the power required, increased maximum forward speed and reduced vibrations. Beside the conventional helicopters, mini and micro unmanned air vehicles have been designed for indoor and outdoor missions.

Recently, researchers have developed increasingly sophisticated mini and micro unmanned aerial vehicles (UAV) particularly for military surveillance applications [1-6]. Mini unmanned air vehicles are used in future for reconnaissance missions where it is undesirable for human beings to go. Rotary air vehicles are preferred to fixed wing air vehicles, particularly when the vehicle is required to remain in hover and maneuver in tightly constrained environments as shown in Figure 1.1. An indoor mission requires a hovering vehicle with good maneuverability characteristics.

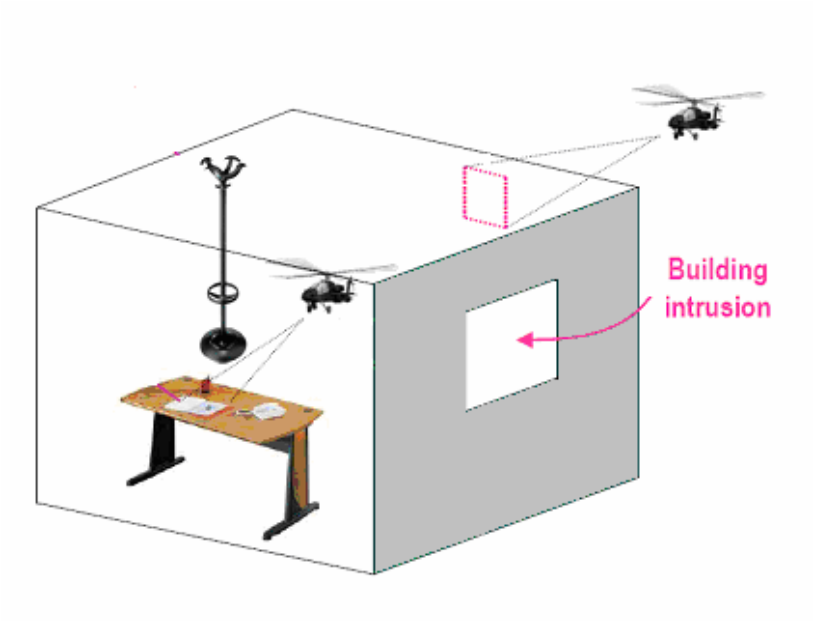

Figure 1.1: UAV Mission Scenario

The vehicle designed in this study is maximum a mini UAV since it has a rotor diameter more than 15 cm and weight more than 100 grams [2, 3]. The mission of this vehicle is indoor optical surveillance. For this type of mission a coaxial helicopter is preferred since coaxial rotor configuration has some advantages over the other configurations.

The most similar designs to this study are AIRSCOOT and HELICOAX [5, 6]. These two models given in Figure 1.2 are similar in terms of their dimensions and technical characteristics, but they have different control systems. AIRSCOOT has control panels on its tail boom for providing yaw motion, whereas HELICOAX has no tail boom and provides yaw motion by the rotor blades.

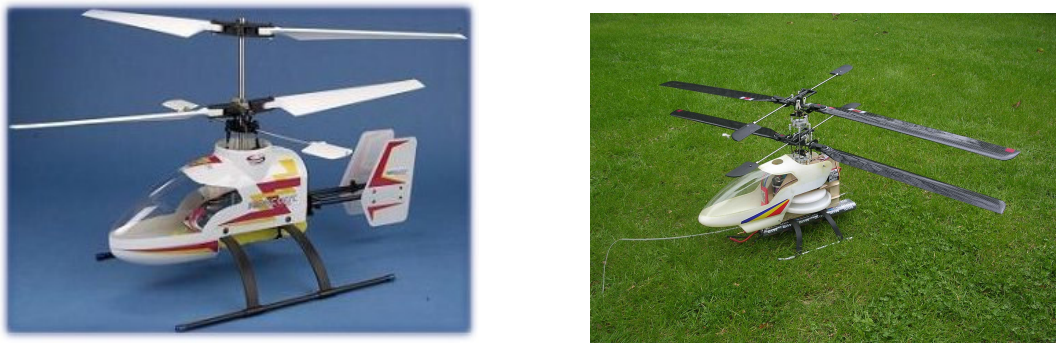

Figure 1.2: AIRSCOOT and HELICOAX [5, 6]

In this study, the design requirements have been determined initially. Design tools have been developed by using “Momentum Theory” and “Blade Element Momentum Theory” to analyze the aerodynamic performance of the vehicle and determine the power needed. The design process is given in Figure 1.3.

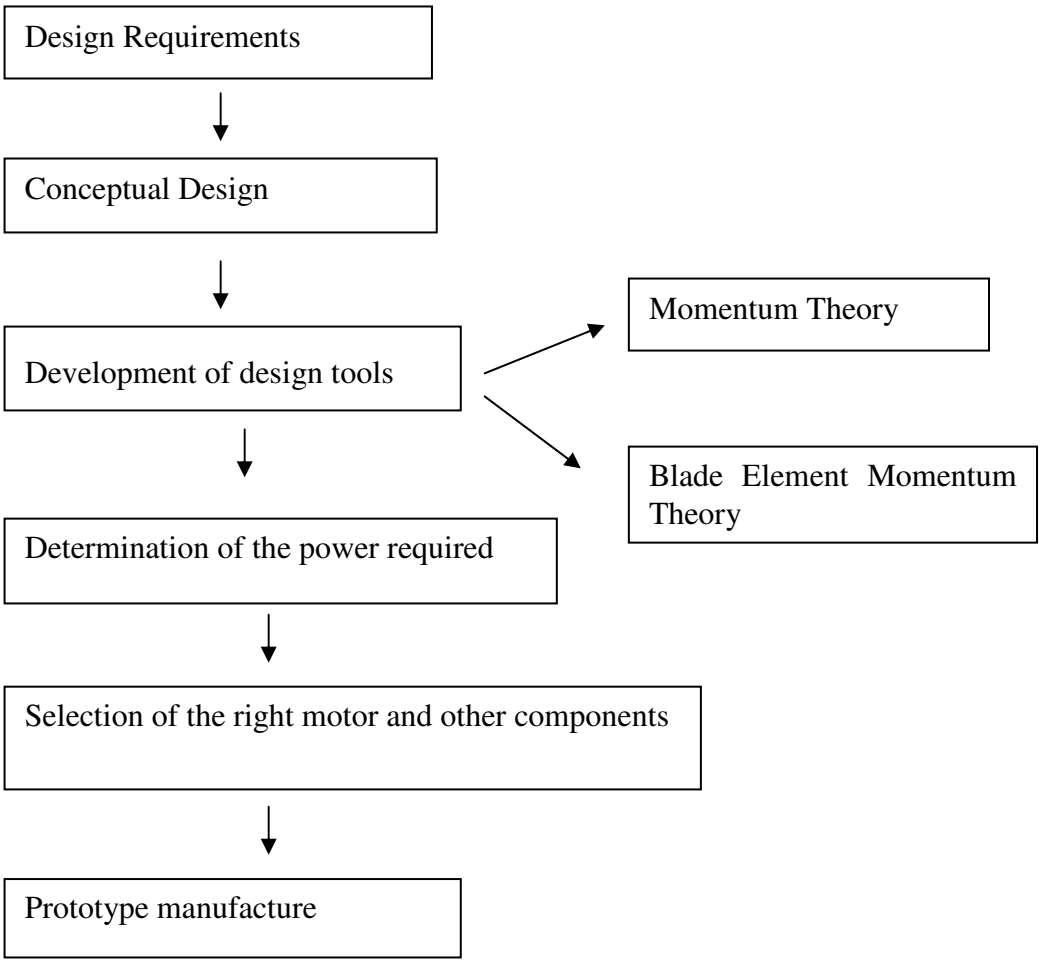

Figure 1.3: Design Process

Another important issue is the control of the helicopter. The lift is provided with the increase of the angular velocities (RPM) of the rotors. The yaw motion of the helicopter can either be provided by using control panels on tail or by changing the pitch angle of the rotor blades without using control panels on tail. Since the vehicle has a single motor, the rpm of the two rotors will be the same therefore it was decided to provide yaw motion by changing the pitch angles of each rotor blades.

1.1 Design Requirements

The baseline design goals are given in Table 1.1. The dimension of the rotor radius is limited for indoor flight environment so that the helicopter can easily fly through windows and doors. The helicopter has 2000 grams of gross weight including payload of about 600-700 grams. The payload consists of a mini camera and autopilot. The estimated duration of the mission is 30 minutes. The mission profile is shown in Figure 1.4.

Table 1.1: Main Design Goals

Rotor Radius	15.24 cm < x < 30 cm
Gross weight	2000 grams
Endurance	30 minutes
Payload (camera+autopilot)	600-700 grams

According to the design requirements the rotor and vehicle configurations have been determined as mentioned in the following sections. The vehicle configuration has been selected according to the hover efficiency, ease of packaging, compactness of folding, simplicity of structure and controllability.

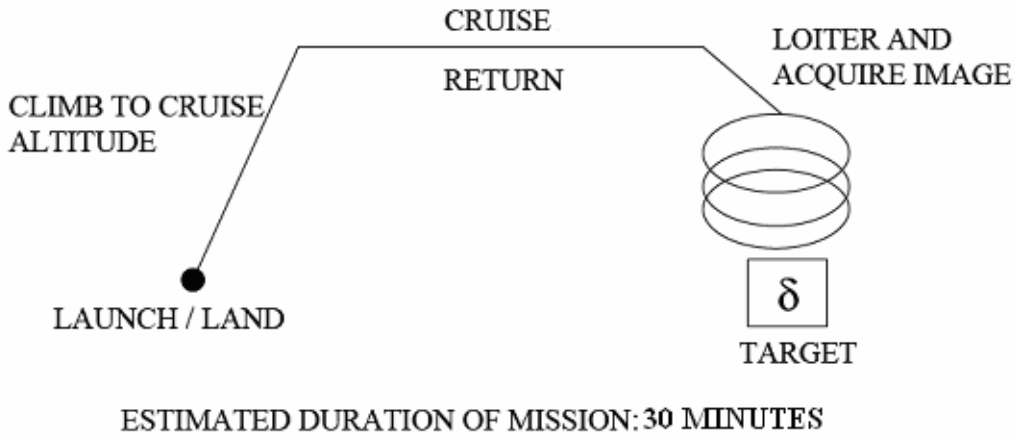

Figure 1.4: Mission Profile

2. CONCEPTUAL DESIGN

During the conceptual design process, the rotor and vehicle configurations have been determined.

2.1 Determining the Rotor Configuration

The rotor configuration has been determined by comparing all the rotor configurations in terms of ease of packaging, compactness of folding, simplicity of structure and controllability.

2.1.1 Single Rotor Configuration

The single rotor configurations or conventional rotors provide anti torque with the tail rotor. This configuration as shown in Figure 2.1 provides good aerodynamic efficiency, controllability and maneuverability. However, compactness of folding due to the tail boom is a disadvantage of this configuration.

Figure 2.1: Single Rotor Configuration [7]

2.1.2 Coaxial Rotor Configuration

This system has two counter rotating rotors located up and down as seen in Figure 2.2. There is no tail rotor since the torque of one of the main rotors cancel the torque of the other's. Due to the torque, the helicopter turns left or right depending on which rotor produces more lift. Mainly, the Russian Kamov helicopters use this rotor configuration.

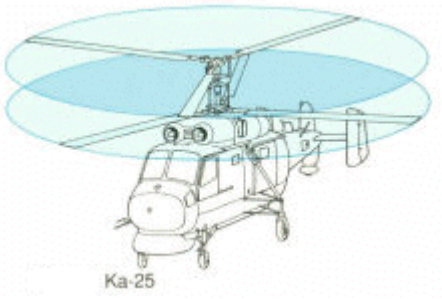

Figure 2.2: Coaxial Rotors [7]

2.1.3 Tandem Rotor Configuration

The torque of each rotor is canceled since the rotors rotate in opposite directions. There are two tandem configurations which have rotors fore and aft as seen in Figure 2.3 and side by side as seen in Figure 2.4.

Figure 2.3: Tandem (fore and aft) Rotors [7]

As an example, the side by side configuration is used by Mil Mi-12 and the fore and aft configuration is used by The Piasecki helicopters. These rotor configurations have much more complicated control systems when compared to a conventional helicopter.

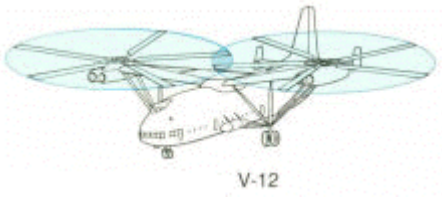

Figure 2.4: Side by Side tandem rotors [7]

2.1.4 Intermeshing Rotor Configuration

This twin non-coaxial rotor configuration which is also called twin intermeshing rotor system is used by H-43 Husky and K-MAX made by the Kaman Company. The intermeshing rotors as shown in Figure 2.5 operate by the same principles as other twin rotor configurations whereas they differ from others by having intermesh rotors mounted very close together.

Figure 2.5: Two Intermeshing Rotors [7]

For a mini unmanned helicopter design, the coaxial design is favored due to having the advantages of compactness of folding, simplicity of structure, and ease of packaging. Also it reduces the net rotor size for a given gross weight and provides anti-torque capability. The fundamental advantage is that the coaxial rotor design allows the aircraft remain small in size due to removal of a tail rotor and boom.

Coaxial design provides increased payload for the same engine power since a tail rotor wastes some of the power that would otherwise be devoted to lift and thrust while with a coaxial rotor design, all of the engine power is devoted to lift and thrust. Reduced noise is another significant advantage of this configuration since there is no interaction between the main and tail rotors. There are also some disadvantages of coaxial rotors such as increase in mechanical complexity due to difficulty in assembling linkages and swashplates (for two rotor discs) around the rotor shaft.

2.2 Determining the Vehicle Configuration

Since the coaxial configuration is employed, there is no tail rotor supported by a tail boom for providing anti torque and yaw stabilization. All power can be devoted to vertical lift. The vehicle mainly consists of coaxial rotor blades, electric motor, battery pack, electronic speed controller, gyroscope, and a mini camera. Both rotors are driven by a single motor. For control of vertical velocity, total thrust is adjusted by varying the motor's rotational speed. The vehicle configuration is shown in Figure 2.6.

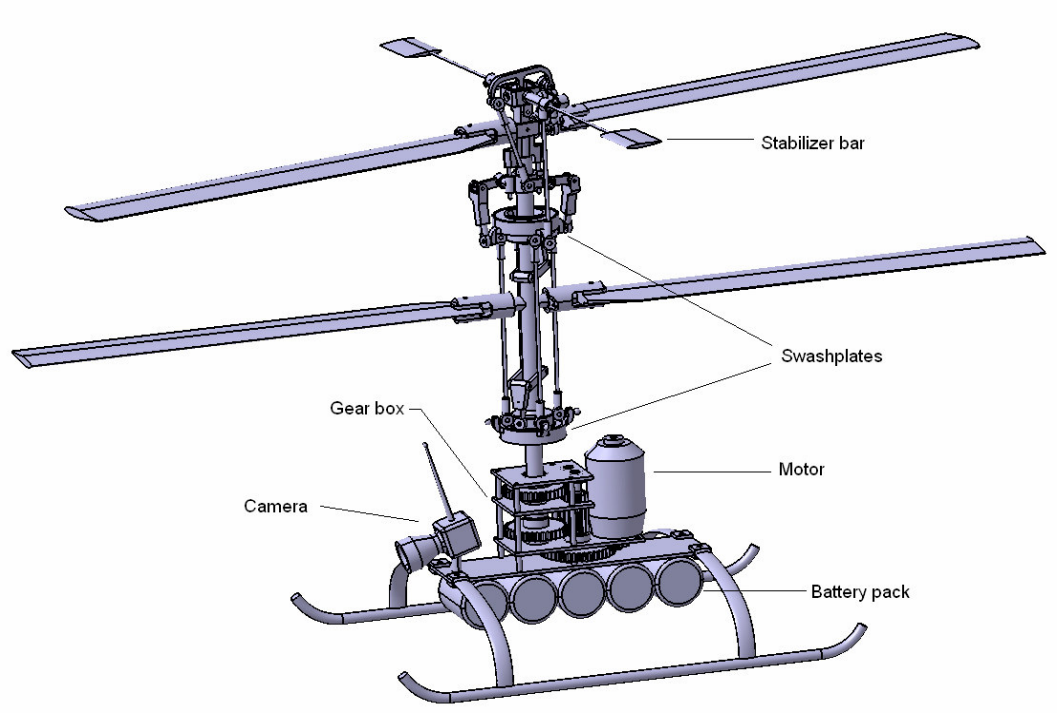

Figure 2.6: System Overview

2.3 Control System

Helicopters generate lift by rotating their rotor through the air. A fixed pitch helicopter as shown in Figure 2.7 ascends when the rotor spins faster, generating more lift and descends as a result of slower rotor rotation which means less lift generation. For collective pitch helicopters, the pitch of the blade effects the lift generation. In this setup, the lift generated can be changed by changing the pitch alone, while the rotor is spinning at a constant speed.

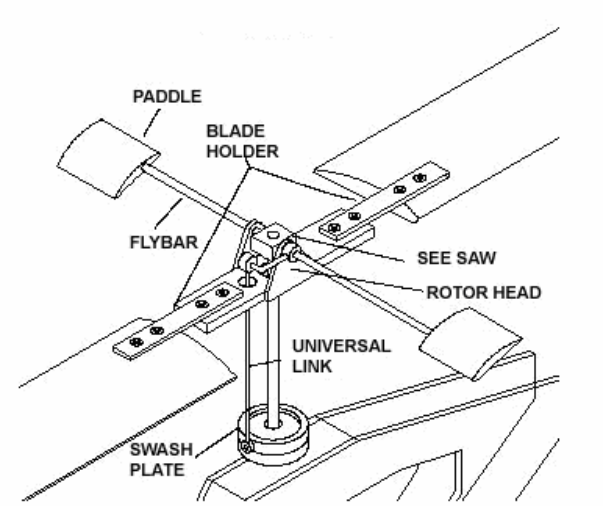

Figure 2.7: Fixed Pitch Type Main Rotor System [8]

A collective pitch helicopter which is shown in Figure 2.8 is more responsive, agile, and smoother to fly. However, they are much harder to learn, require a more complicated transmitter, and cost much more than fixed pitched helicopters. On the other hand, they have more moving parts, which facilitates breaking and complicates the maintenance. A fixed pitch helicopter is easier to fly, since it has fewer moving parts, and requires less maintenance.

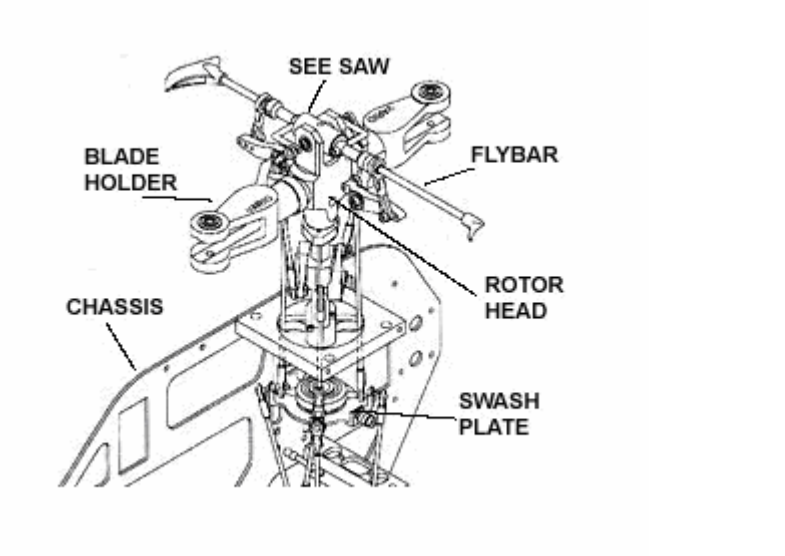

Figure 2.8: Collective Pitch Type Main Rotor System [8]

First, it was decided to design a collective pitch type helicopter. With a fixed pitch helicopter lift is generated by increasing rotor speed and yaw motion is supplied by slowing or speeding up one of the two rotors whereas with a collective pitch helicopter lift and other maneuvers are generated and altered by changing only the pitch angle of the blades. Fixed pitch helicopter leads to sudden changes in rotor speed which means consuming high energy. However, it is not a big problem in small scale helicopters. If a collective pitch type helicopter is designed, it will be difficult to generate yaw motion by changing the pitch angle of both rotors which are connected mechanically each other.

The advantages of both systems have been considered during the design of the helicopter.

3. PRELIMINARY and DETAILED DESIGN of a COAXIAL HELICOPTER

The aerodynamic performance of a coaxial rotor system can initially be examined by using the momentum theory which is applied to a control volume of coaxial rotors as shown in Figure 3.1. The results of the Momentum Theory are then compared with the results of the Blade Element Momentum Theory.

A gross weight of approximately 2000 g was set as the target weight for the preliminary design.

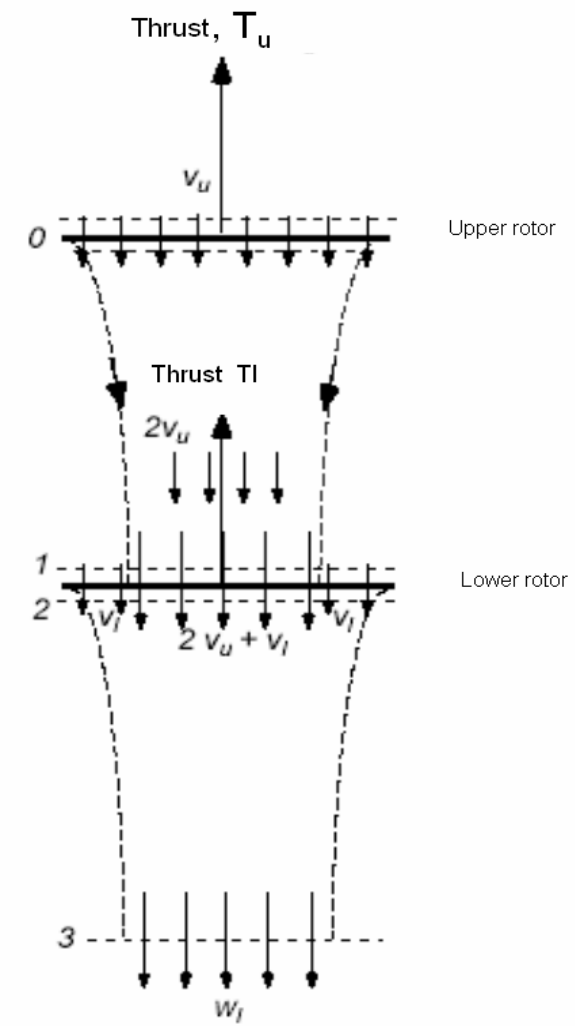

Figure 3.1: Coaxial Rotor System With the Lower Rotor Operating in the Vena Contracta of the Upper Rotor [9]

3.1 Application of the Momentum Theory

For coaxial rotor systems, the momentum theory is applied for different cases. For the first case, it is assumed that the rotors rotate very closely (or in the same plane) having the same thrust or as in the second case they rotate in the same plane having equal and opposite torque. In the third case, the rotors operating at the same thrust are spaced sufficiently far apart that the lower rotor operates in the vena contracta of the upper rotor. In the fourth case, the rotors operating at balanced torque are spaced sufficiently far apart with the lower rotor operating in the vena contracta of the upper rotor [9]. In order to choose the optimum rotor configuration, the induced power losses must be taken into account for each case. For the first two cases the induced power factor is 1.414, whereas for the third and fourth cases the induced power factors are 1.281 and 1.219, respectively [9]. When the induced power factors are compared, it is seen that the assumption made in the fourth case represents the minimum power loss. Moreover, since the conventional coaxial rotors are spaced sufficiently far apart to prevent inter-rotor blade collisions, the flow model for this case is much more realistic than the other cases. Thus, in this study, the momentum theory has been applied with the assumption of separated rotors operating at balanced torque as mentioned in the fourth case.

The calculations made on both upper and lower rotors are for hover condition. According to the 4^{th} case, it is assumed that there is an equal balanced torque between the upper and lower rotors. Then $P_u = P_l$ which leads to

$$T_u v_u = T_l (v_u + v_l) \tag{3.1}$$

3.1.1 Upper Rotor Analysis

The mass flow rate over the upper rotor is

$$\dot{m}_u = \rho A v_u \tag{3.2}$$

The thrust on the upper rotor is

$$T_u = (\rho A v_u).2v_u \tag{3.3}$$

The work done by the upper rotor is

$$P_u = (2\rho A {v_u}^2) v_u = 2\rho A v_u^3 \tag{3.4}$$

3.1.2 Lower Rotor Analysis

One-half of the disk area of the lower rotor operates in the slipstream velocity induced by the upper rotor.

The mass flow rate over the inner and outer parts of the lower rotor is

$$\dot{m}_l = \rho\left(\frac{A}{2}\right)(2v_u + v_l) + \rho\left(\frac{A}{2}\right)v_l = \rho A(v_u + v_l) \tag{3.5}$$

The first term of the left sight of the equation represents the mass flow rate over the inner part and the second term represents the mass flow rate over the outer part of the lower rotor.

The thrust on the lower rotor is calculated by using the following formula

$$T_l = \rho A(v_u + v_l)w_l - 2\rho A v_u^2 \tag{3.6}$$

The work done by the lower rotor is

$$P_l = T_l(v_u + v_l) \tag{3.7}$$

Substituting Equation 3.6 into Equation 3.7 and rearranging gives

$$P_l = \rho A(v_u + v_l)^2 w_l - 2\rho A v_u^2(v_u + v_l) \tag{3.8}$$

Multiplying both sides of the Equation 8 by v_u and remembering that $P_u = P_l$ leads to

$$2P_l v_u = \rho A(v_u + v_l)^2 v_u w_l - 2\rho A v_u^3 v_l \tag{3.9}$$

Which leads to

$$P_l(2v_u + v_l) = \rho A(v_u + v_l)^2 v_u w_l \tag{3.10}$$

The work done by the lower rotor is equal to the gain in kinetic energy of the slipstream, hence

$$T_l(v_u + v_l) = \frac{1}{2}\rho A(v_u + v_l)w_l^2 - \frac{1}{2}\rho\left(\frac{A}{2}\right)(2v_u)(2v_u^2) \tag{3.11}$$

Using Equation 3.7, and rearranging Equation 3.11 gives,

$$P_l = \frac{1}{2}\rho A(v_u + v_l)w_l^2 - 2\rho A v_u^3 \tag{3.12}$$

Since $P_u = P_l$,

$$2P_l = \frac{1}{2}\rho A(v_u + v_l)w_l^2 \tag{3.13}$$

The work done by the lower rotor is then,

$$P_l = \frac{1}{4}\rho A(v_u + v_l)w_l^2 \tag{3.14}$$

Substituting Equation 3.14 into Equation 3.10 and rearranging gives

$$w_l = 4v_u\left(\frac{v_u + v_l}{2v_u + v_l}\right) \tag{3.15}$$

Again, $P_u = P_l$ and substituting Equation 3.15 into Equation 3.7 gives the following cubic equation

$$2v_l^3 + 5v_u v_l^2 + 2v_u^2 v_l - 2v_u^2 = 0 \tag{3.16}$$

Numerical solution of Equation 3.16 leads to

$$v_l = 0,4375v_u \tag{3.17}$$

Substituting Equation 3.17 into Equation 3.15 gives

$$w_l = 2,359v_u \tag{3.18}$$

As mentioned previously, a gross weight of approximately 2000 g was set as the target weight. Equations 3.17 and 3.18 lead to adjusting the thrust on the upper and lower rotors as so the total thrust corresponds to 2000 grams gross weight. The work done by the upper and lower rotor is then calculated.

The ideal power and required total power values have been calculated using the equations given above and are shown in Table 3.1 The total required power is 310.8 W.

Table 3.1: Power Values of the Upper and Lower Rotors

	Upper Rotor	**Lower Rotor**
P_{ideal}	51,6 W	51,6 W
P_{actual} (FM=0.5)	103,2 W	103,2 W
Motor power (eff=0.83)	124,3 W	124,3 W
For maneuver (1.25x)	155,4 W	155,4 W

3.2 Application of the Blade Element Momentum Theory

Blade Element Momentum Theory is used to simplify the analysis of a 3 dimensional flow over a wing. According to the theory, it is assumed that the wing can be thought of as being composed of a large number of wing sections, which are obtained when a wing is cut up by a large number of planes normal to the wing span axis. Each wing section or element can be thought of as being a very small part of an infinitely long 2-dimensional aerofoil of the same cross-sectional shape as shown in Figure 3.2. It is assumed that the flow is locally 2-dimensional which means the flow over each wing section is assumed to be independent of what is happening elsewhere over any of the other section.

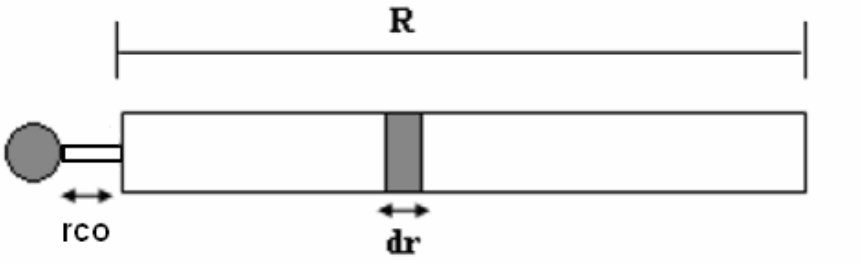

Figure 3.2: Blade Element Top View

In this study, BEMT is used for rotor performance calculations. This theory helps to calculate iteratively the performance parameters such as lift and drag forces, power, thrust, and torque over the blade sections. The calculations are made for hover condition.

It is assumed that each rotor blade is composed of 20 equally divided wing sections.

The thickness of each element is

$$dy = \frac{R - rco}{20} \tag{3.19}$$

The distance of each element to the hub

$$y = rco + dy.n_x \tag{3.20}$$

The non dimensional forms of the thickness and distance to the hub of each element are given in Equation 3.21 and 3.22, respectively.

$$r = \frac{rco}{R} + \frac{dy}{R} n_x \tag{3.21}$$

$$dr = \frac{1 - rco/R}{20} \tag{3.22}$$

In order to make a realistic analysis, the calculations are made on upper and lower rotors separately.

3.2.1 Upper Rotor Analysis

To calculate the aerodynamic forces such as lift and thrust provided by each rotor blade, the inflow ratio must be calculated initially. The inflow ratio on the upper rotor is

$$\lambda(r_n) = \frac{\sigma C_{l\alpha}}{16}\left[\sqrt{1 + \frac{32}{\sigma C_{l\alpha}}\theta_u(r_n) r_n} - 1\right] \tag{3.23}$$

Since the following formula includes the induced velocity term, the thrust coefficient can be written depending on the inflow ratio as given in Equation 3.25.

$$dT_u = (2\rho v_u dA) v_u = 4\pi\rho v_u^2 y dy \tag{3.24}$$

The thrust coefficient on the upper rotor is

$$dC_{Tu} = 4\lambda^2 r dr \tag{3.25}$$

The work done by the upper rotor is

$$dC_{Pu} = \lambda dC_{Tu} = 4\lambda^3 r dr \tag{3.26}$$

By integrating the Equations 3.25 and 3.26 over the blade gives the thrust and power values. Since the thrust is equal to the lift in hover condition, the lift provided by

each rotor blade can be estimated by integrating the thrust coefficient through the blade by using the BEMT or the lift coefficient can be directly calculated and integrated over the blade. Table 3.2 summarizes the estimation of the thrust coefficient by using the Equations given above.

Table 3.2: Thrust coefficient distribution along the upper rotor blade

r	dr	λ(r)	CTu
0,145	0,045	0,037848	3,74E-05
0,19	0,045	0,046113	7,27E-05
0,235	0,045	0,053617	0,000122
0,28	0,045	0,060538	0,000185
0,325	0,045	0,066995	0,000263
0,37	0,045	0,073069	0,000356
0,415	0,045	0,078822	0,000464
0,46	0,045	0,0843	0,000588
0,505	0,045	0,089538	0,000729
0,55	0,045	0,094566	0,000885
0,595	0,045	0,099408	0,001058
0,64	0,045	0,104082	0,001248
0,685	0,045	0,108604	0,001454
0,73	0,045	0,11299	0,001678
0,775	0,045	0,117249	0,001918
0,82	0,045	0,121394	0,002175
0,865	0,045	0,125432	0,00245
0,91	0,045	0,129371	0,002741
0,955	0,045	0,133218	0,003051
1	0,045	0,13698	0,003377
			0,024851

As seen from Table 3.2, integrating the thrust coefficient over the blade gives the thrust coefficient which is 0.025. This value coincides the value calculated using the Momentum Theory which is 0.023. The thrust distribution over the blade can be seen in Figure 3.3.

The lift supplied by the upper rotor is,

$$P = C_P\left(\frac{1}{2}\rho V^3 A\right) \tag{3.27}$$

To get a result in terms of weight carried by each of the upper rotor blades,

$$L = (6.30\times 9,81)/1000 \simeq 643 \text{ grams} \tag{3.28}$$

Which means each of the upper rotor blades carry 643 grams.

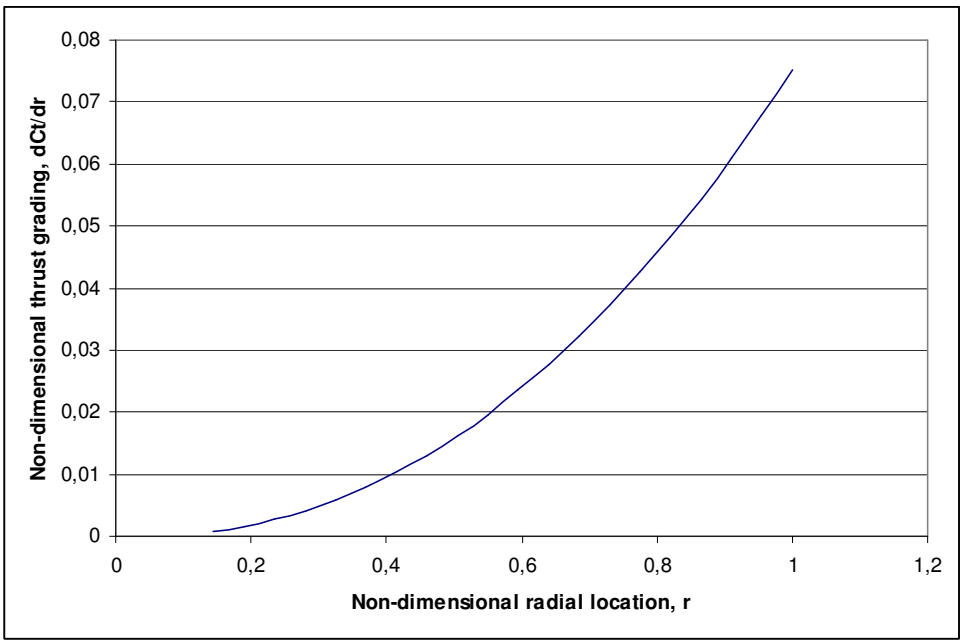

Figure 3.3: Distribution of thrust on upper rotor blade

As mentioned before, the lift coefficient can be found directly by using the lift coefficient as shown in Table 3.3.

Table 3.3: Lift coefficient distribution along the upper rotor blade

α(rad)	Clα	dCl
0,143624934	5,73	0,822971
0,160854141	5,73	0,921694
0,174632032	5,73	1,000642
0,186018449	5,73	1,065886
0,1956588	5,73	1,121125
0,203973831	5,73	1,16877
0,211252211	5,73	1,210475
0,217700049	5,73	1,247421
0,223469294	5,73	1,280479
0,228674958	5,73	1,310308
0,233406029	5,73	1,337417
0,23773267	5,73	1,362208
0,241711094	5,73	1,385005
0,245386977	5,73	1,406067
0,248797897	5,73	1,425612
0,251975103	5,73	1,443817
0,254944843	5,73	1,460834
0,25772935	5,73	1,476789
0,260347614	5,73	1,491792
0,262815967	5,73	1,505935

The lift provided by each of the upper rotor blades is,

$$L = C_{l_u}\left(\frac{1}{2}\rho V^2 n.c.dy\right) \tag{3.29}$$

Calculation of the inflow ratio also leads to determination of the total power required by first calculating the ideal power value using Equation 3.26 and 3.27.

$$2P_{ideal} = 2C_P\left(\frac{1}{2}\rho V^3 A\right) = 123.05 \text{ W} \tag{3.30}$$

Since FM = 0.5,

$$P_{actual} = P_{ideal} / FM = 246.1\,\text{W} \tag{3.31}$$

For a motor power efficiency of 83 % and for maneuver the total power required is calculated. The total power required for the upper rotor (which is equal to the power of lower rotor) calculated by using the Momentum Theory and Blade Element Momentum Theory is given in Table 3.4.

Table 3.4: Momentum Theory and BEMT results for power values of upper rotor.

	Momentum Theory	**BEMT**
Power required (total)	206,4 W	246,1 W
Motor power (eff=0.83)	248,6 W	296,5 W
For maneuver (1.25x)	310,8 W	370,7 W

Determination of the power required is important while selecting the convenient motor.

3.2.2 Lower Rotor Analysis

The lower rotor operates in the vena contracta of the upper rotor. The contracted area is as in the Figure 3.4.

The contracted wake area is

$$A_c = \pi r_c^2 \tag{3.32}$$

Where,

$$r_c = 2^{-1/2} = 0,707 \text{ or } \frac{A}{A_c} = 2 \tag{3.33}$$

Due to the contracted area, for the lower rotor, the inflow ratio and lift coefficient are calculated both on the contracted (inner) and outer parts of the rotor area. The inflow ratio leads to calculation of the thrust and power coefficients.

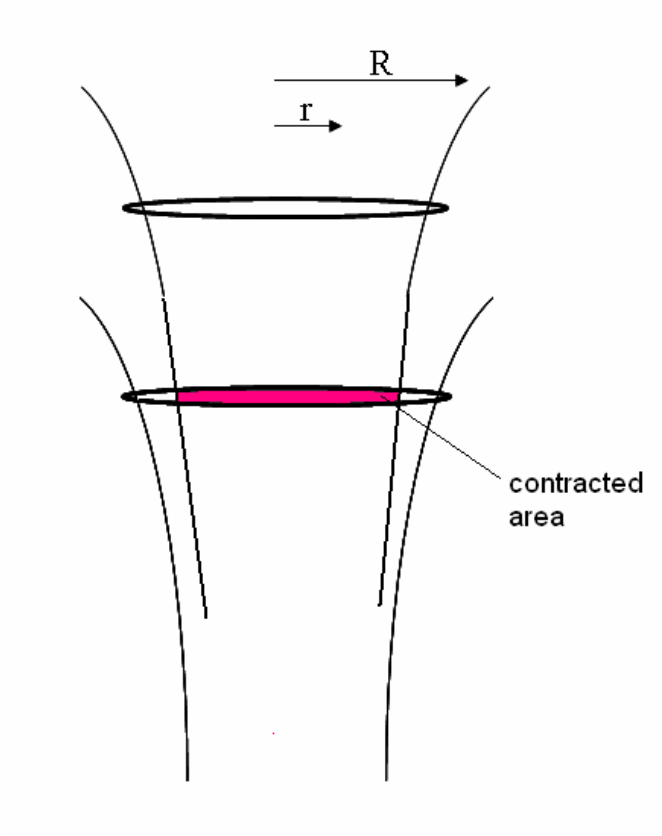

Figure 3.4: The Area Under Fully Developed Slipstream of the Upper Rotor

The inflow ratio on the lower rotor for points on the disk within the slipstream area from the upper rotor is calculated using the equation given below

$$\lambda(r_n) = \sqrt{\left(\frac{\sigma C_{l\alpha}}{16}\right)^2 - \left(\frac{(A/A_c)\lambda_u}{2}\right)^2 + \frac{\sigma C_{l\alpha}}{8}\theta_l r} - \left(\frac{\sigma C_{l\alpha}}{16} - \frac{(A/A_c)\lambda_u}{2}\right) \tag{3.34}$$

The inflow ratio on the lower rotor for points outside the area that are unaffected by the upper rotor is

$$\lambda(r_n) = \sqrt{\left(\frac{\sigma C_{l\alpha}}{16}\right)^2 + \frac{\sigma C_{l\alpha}}{8}\theta_l r} - \left(\frac{\sigma C_{l\alpha}}{16}\right) \tag{3.35}$$

The lift coefficient on the inner (contracted) part is

$$dC_{T_{l1}} = \frac{2w_l(v_{u+}v_l)}{(\Omega R)^2} rdr \tag{3.36}$$

The lift coefficient on the outer part is

$$dC_{T_{l2}} = \frac{2\rho v_u^2 dA}{\rho\pi R^2(\Omega R)^2} = 4\lambda rdr \tag{3.37}$$

The similar calculations as in the previous section are done for the lower rotor.

4. COMPONENTS AND TAKEOFF WEIGHT

One advantage of a UAV design over conventional full scale aircraft design is that the calculation of take off weight can be performed with relatively little use of empirical data. This is due to the fact that most of the components to be carried, as well as their size and weight, are known. However, the disadvantage is that the vehicle must be designed to adjust these components. For the design of the helicopter, the components to be carried are fundamentally power system, batteries, video camera and transmitter, radio control receiver, gyro and other components.

4.1 Power System

The power needed for the optimum rotor design has been determined by using both the Momentum and Blade Element Momentum Theories.

Power from an engine must be transmitted to the rotor shaft to turn the rotor. The power is provided by an electric motor. The electric motor has been selected according to the power needed to supply enough thrust in the hover condition, since the maximum power is required during hover.

While selecting the right motor it should be taken into account that a motor which is too small will over heat and ruin itself whereas a motor which is too large will be a detriment to performance, due to the added weight. Using single motor is cheaper, lighter; but also there is a need for an inverter and a bigger motor. On the other hand, using double motor is more expensive, and the control of two motor is much more complicated when compared to single motor [10]. Using single motor facilitates the control of the helicopter although it is a more complicated configuration. Therefore, it was decided to use single motor instead of double motor.

A brushless DC motor was preferred, since it has several advantages over other electric motors, such as higher efficiency and reliability, longer lifetime, and reduced noise. Brushless DC motors are more powerful than AC as well as brush DC motors, and are capable of very high speeds and torque. They can operate in a wider temperature range, since they have a lower thermal resistance. Moreover, having a

higher torque to inertia ratio, high starting energies, and high breakaway torques make them more efficient than typical AC induction motors and DC motors. The lack of brushes allows them to have a high speed range. Therefore, brushless DC motors have complex motion control capabilities.

Having decided on using a brushless motor it should also be decided to use whether an outrunner motor which has stationary coils at the center and rotating magnet on the outside or inrunner motor which has stationary coils surrounding the rotating magnet at the center. An outrunner motor is simpler, quieter, and prevents heating problem hence a brushless outrunner motor is more convenient for this design.

Motor RPM determines the specific motor and battery choice, by the following approximate formula (assuming lithium polymer batteries).

Motor RPM = 0.8 x 3.5V x Series Cell Count x Motor kV Rating (4.1)

The right motor and battery combination should be selected in order to satisfy the motor RPM formula. It can be done with a low kV motor and a high series cell count battery, or vice versa [11].

Figure 4.1: Axi 2826/8 Brushless Electromotor [11]

The motor that will be used is shown in Figure 4.1, and the fundamental technical specifications are given in Table 4.1.

Table 4.1: Technical Specifications of the Electric Motor

RPM/V	1130
Max. Efficiency	83 %
Max. efficiency current	25 - 37 A (> 75 %)
Current capacity	55 A / 60 s
No load current	2,9 A
Internal Resistance	30 mΩ
No. Of cells	3-4
Dimensions (ϕ x L)	35x54 mm
Shaft diameter	5 mm
Weight with cables	181 g

The RPM and output power values altering with the current is given in Figure 4.2.

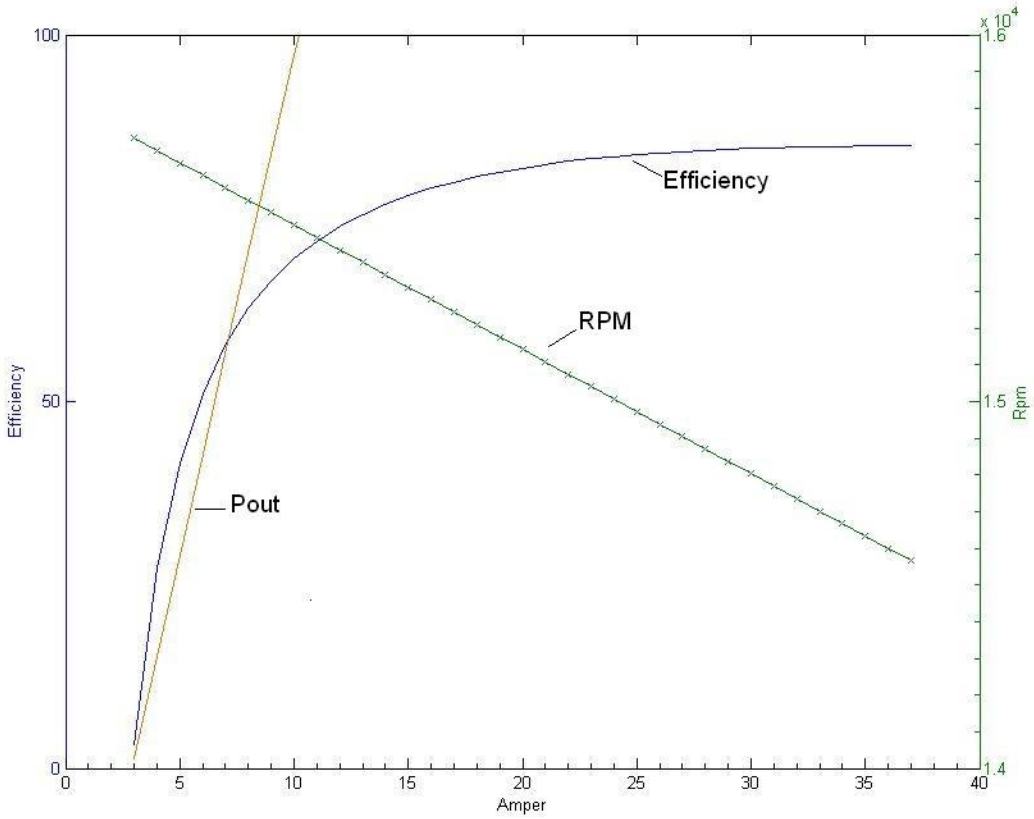

Figure 4.2: RPM and Output Power Altering with the Current

4.2 Rotor Blades

Two blades with NACA 0012 airfoil sections are selected. These blades provide enough lift to fly the helicopter which has 2000 grams gross weight.

The lift that each blade element is supposed to carry is determined by using the Blade Element Momentum Theory, as mentioned in chapter 3. As a result of the Blade Element Momentum Theory, each of the upper rotor blades supplies 643 grams of lift which satisfies the value already calculated by the Momentum Theory. The lift provided by upper and lower rotors is summarized in Table 4.2.

Table 4.2: The lift supplied by the upper and lower rotor

	Momentum Theory	**BEMT**
Lift of each blade of upper rotor	2 x 590 grams	2 x 643 grams
Lift of each blade of lower rotor	2 x 410 grams	2 x 364 grams
TOTAL	2000 grams	2014 grams

The blades that will be used are made of carbon fiber composites since they have light weight, high performance, high stiffness, and reliability. The blades are shown in Figure 4.3.

Figure 4.3: Carbon Fiber Composite Blades

4.3 Camera

The camera and video transmitter used were the smallest and lightest that could be found within limitations. The camera and transmitter has a mass of 9 grams and operates on 2.4 GHz. The actual camera that will be used is shown in Figure 4.4.

Figure 4.4: Camera and Transmitter

4.4 Battery Pack

A battery pack is usually composed of two or more cells put together in series for increased voltage, or in parallel for increased capacity. There are different kinds of battery pack such as LiPo, NiMH, and NiCd pack. Lithium polymer battery pack, are ideal for use with brushless motors in radio controlled airplanes and helicopters due to their low weight and high capacity compared to NiMH and NiCd packs. The selected battery as shown in Figure 4.5 is able to provide 4500 mA current.

Figure 4.5: Li-Po Battery Pack

Batteries are relatively heavy and system weight does not decrease during flight. Motor speed is controlled by varying the voltage applied to the motor. Endurance and range depend upon current requirements and battery capacity.

Along with a brushless motor and battery, also there will be a need for a brushless speed control (ESC) as shown in Figure 4.6 with an amp rating equal to or greater than the peak current drawn by the selected motor. Other items such as speed controller, servo receiver and gyro are also shown in Figure 4.6. Radio control receiver has a mass of 8 grams and operates on 72 MHz [11].

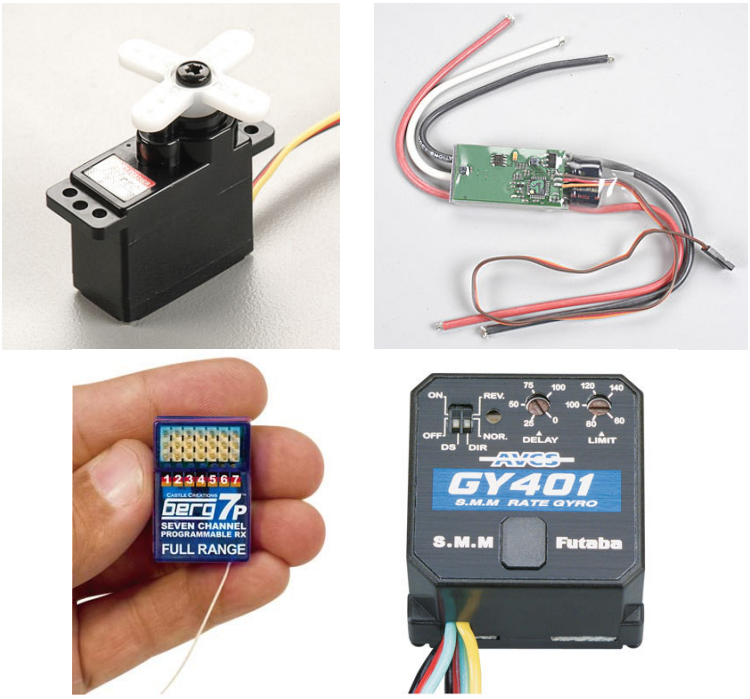

Figure 4.6: Servo, ESC, receiver, and Gyro

5. WEIGHT AND COST ANALYSIS

In this section the weight and cost analysis have been done. These analysis can be useful to estimate the weight and cost for the design of similar vehicles in further studies.

5.1 Mass Breakdown

The components and mass breakdown of the components are given in Table 5.1, and Figure 5.1 respectively.

Table 5.1: Components and Masses [10]

Component	Mass/Item (g)	#	Total
Motor	181	1	181
Li-Po Battery	450	1	450
Speed Control	58	1	58
Servo	11	3	33
Rotor blades	12	4	48
RC receiver	8	1	8
Gyro	27	1	27
Payload	600	1	600
Structure	595	1	595
Total			**2000**

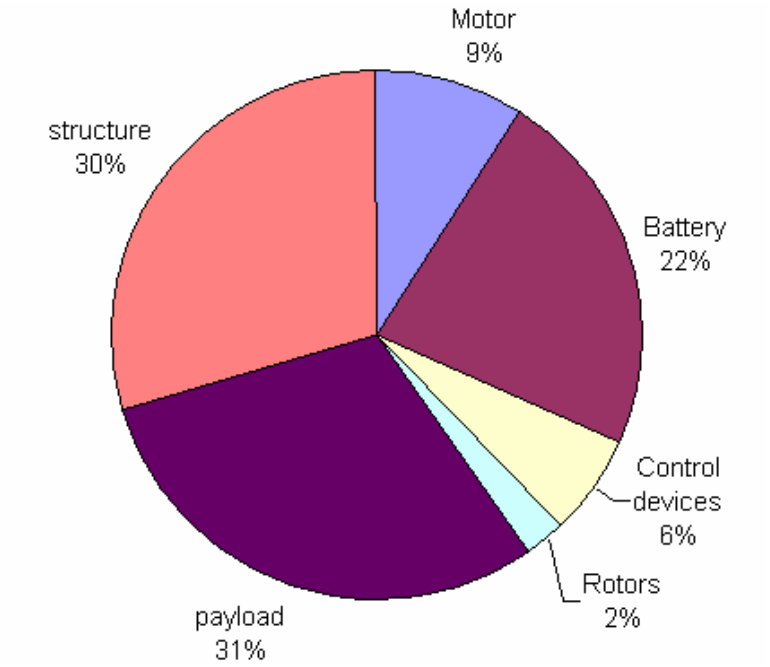

Figure 5.1: Mass Breakdown

5.2 Cost Analysis

The budget for this project was supplied by ROTAM. Currently, $800 has been spent for this study. No external funds were received for the finances of this project. A table of specific costs are summarized in Table 5.2.

Table 5.2: Cost Breakdown

Component	Number of Units	Unit Cost	Total Cost
Carbon Blades	4	$31,99	$127.96
Flybar	1	$3.49	$3.49
Swashplate	2	$84,99	$169.98
Washout Set	1	$14.99	$14.99
Plastic links pack	2	$20,99	$41.98
Gyro	1	$139.99	$139.99
Electric motor	1	$93,80	$93.80
120^0 swashplate	1	$13,99	$13.99
ESC	1	$118.99	$118.99
Shipping			$14.99
UPS			$59.98
Total			$800.14

6. CONCLUSION

A mini helicopter with a maximum take of weight of 2000 grams is designed. The mission of the helicopter is indoor surveillance with an endurance of 30 minutes. The technical specifications of the helicopter is given in Table 6.1.The body of the helicopter is constructed and COTS components are procured. The system integration, ground and flight tests will be performed.

Table 6.1: Design Characteristics

Description	
Design	**HelyScout**
Type	Unmanned Coaxial RC Helicopter
Mission	Indoor Optical Surveillance
Specs	
Number of rotors	2
Main rotor diameter	0.6 m
Number and type of engine	Single, brushless electric motor
Engine max. power	429,94 W
Battery	4500 mAh Li-Po
Max. takeoff weight	2000 g
Empty weight	1400 g
Max. endurance with normal payload	30 minutes

REFERENCES

[1] **Bouabdallah S., Siegwart R., and Caprari G.,** 2006, Design and Control of an Indoor Coaxial Helicopter, *International Conference on Intelligent Robots and Systems*, October 9-15.

[2] **Grasmeyer, J. M., and Keennon M.T.,** 2001, Development of the Black Widow Micro Air Vehicle, *American Institute of Aeronautics and Astronautics, AIAA Paper*, **AIAA -2001-0217**.

[3] **Davis W.R, Kosicki Jr. B.B., Boroson D. M., and Kostishack D. F.,** 1996, Micro Air Vehicles for Optical Surveillance, *The Lincoln Labaratory Journal*, Volume **9**, Number 2.

[4] **Bohorquez F., Samuel P., Sirohi J., and Couch R.,** 2005, Design and Testing of a Rotary Wing MAV with an Active Structure for Stability and Control, *AHS 61st Annual Forum,* Grapevine, TX, June 1-3.

[5] *On-line Documentation*: www.airscoot.com

[6] *On-line Documentation*: http://users.skynet.be/thididag/helicoax/Helicoax.htm

[7] *On-line Documentation*: http://www.helis.com/howflies/rotconf2.php

[8] *On-line Documentation*: http://www.electric-rc-helicopter.com/article/fixed_collective_pitch.php

[9] **Leishman, J.G., and Ananthan S.,** 2006, Aerodynamic optimization of a Coaxial Proprotor, *62th Annual Forum and Technology Display of the AHS International*, Phoenix, AZ, May 9-11.

[10] **Stauffer, Y.,** 2004, Coaxial Helicopter Design, *Master Thesis*, Ecolé Polytechnique Federale de Lausanne, Institute D'ingenierie Des Systemes, Lausanne.

[11] **Erzincanlı, B., and Aslan, A.R.**, 2007, Design and Performance Analysis of a Mini Unmanned Coaxial Helicopter, *Ankara International Aerospace Conference, Ankara, Turkey*, September 10-12.

RESUME

Belkıs ERZİNCANLI was born in İstanbul, Turkey in 1982. She had her high school education in Uskudar Science High School (UFL). She graduated from Aeronautical Engineering Department, Faculty of Aeronautics and Astronautics of Istanbul Technical University in 2005. She is a graduate student of Aeronautics and Astronautics Engineering M.Sc program in ITU. She is currently a research assistant in the same faculty of ITU.